Eur Radiol (2005) 15: 2396–2403
DOI 10.1007/s00330-005-2816-8

Srinivasan Harish
Asif Saifuddin

Imaging features of spinal osteoid osteoma with emphasis on MRI findings

Received: 2 March 2005
Revised: 30 April 2005
Accepted: 9 May 2005
Published online: 23 June 2005

S. Harish (✉) · A. Saifuddin
Department of Radiology,
Royal National Orthopaedic
Hospital NHS Trust,
Stanmore,
Middlesex, HA7 4LP, UK
e-mail: sharish@doctors.net.uk
Tel.: +44-20-89095443
Fax: +44-20-89095281

A. Saifuddin
Institute of Orthopaedics and
Musculoskeletal Sciences,
University College London,
London, UK

Abstract A retrospective evaluation of the imaging of 13 patients with a diagnosis of osteoid osteoma (OO) of the spine was undertaken. Available imaging included radiographs (n=10), computed tomography (CT) (n=13), bone scintigraphy (n=5) and magnetic resonance imaging (MRI) (n=13). MRI features evaluated were pattern of neural arch and vertebral body oedema and the presence of an identifiable nidus. MRI features were correlated with other available imaging. There were seven males and six females with an age range of 8–59 years. On radiographs, scoliosis was present in ten and a sclerotic pedicle in nine patients. Focal increased uptake on bone scintigraphy consistent with OO was seen in all five patients where scintigraphy was available. On CT, a nidus was identified in all patients and reactive sclerosis was seen in 12. MRI demonstrated the nidus in eight patients and unilateral neural arch oedema with anterior extension to involve the ipsilateral posterolateral vertebral body in 11. When MRI is performed in the evaluation of back pain, the presence of unilateral neural arch oedema extending to involve the posterolateral vertebral body raises the possibility of spinal OO and should prompt CT to confirm the presence of a nidus.

Keywords Spine · Osteoid osteoma · MRI · CT · Radiographs · Scintigraphy

Introduction

Osteoid osteoma (OO) of the spine is a relatively rare tumour, which should be included in the differential diagnosis of any young patient with back pain, scoliosis or pain referred to the lower limb [1–3]. Prompt diagnosis is important to reduce the duration of symptoms and the risk of structural spinal deformity. Magnetic resonance imaging (MRI) features of appendicular OO are well described in the literature [4, 5]. We describe the characteristic imaging features of spinal OO in 13 cases and underline the importance of considering this diagnosis in patients referred for MRI with vague symptoms of back pain in whom OO is unsuspected.

Materials and methods

A retrospective review of the available imaging on 13 patients with a diagnosis of spinal OO who presented to our institution over a 4-year period was undertaken. There were seven males and six females with a mean age of 20 (range 8–59) years. All patients presented with back pain. Radiographs were available in ten patients, and 99^{m}-technetium methylene diphosphonate (99^{m}-Tc MDP) bone scintigraphy was performed in five patients. All 13 patients had computed tomography (CT) and MRI. MRI sequences included various combinations of T1-weighted spin-echo (SE) and T2-weighted fast-spin-echo (FSE) sequences in the sagittal, axial and coronal planes. In one case, gadolin-

ium was administered. Direct histological confirmation of the lesion was available in six patients. The remaining seven patients had lesions with characteristic appearances of OO on CT, with a demonstrable nidus having central mineralisation, allowing a confident radiological diagnosis to be made. Spontaneous clinical resolution occurred in one of these seven patients. In three patients who were originally referred from outside hospitals, clinical follow-up was not available. In the remaining three patients, treatment had not been instituted.

The following imaging features were analysed for each case: Radiographs—presence of scoliosis and neural arch sclerosis; CT—presence and location of nidus and sclerosis; bone scintigraphy—presence of focal intense uptake typical of OO; MRI—presence and pattern of neural arch and vertebral body oedema (grade, distribution and extent), presence of an identifiable nidus and abnormality of the paraspinal or epidural space. Grading of the oedema pattern was based on a previously described system [5] as follows:

Grade 1: no perinidal oedema
Grade 2: thin rim of perinidal oedema
Grade 3: oedematous change circumferentially distributed around the nidus
Grade 4: extensive oedema more than in grade 3 with or without involvement of adjacent soft tissues

Results

Patient age and gender and location of the nidus and MRI features are presented in Table 1.

Radiographs

Scoliosis was demonstrated along with a sclerotic and/or indistinct pedicle on frontal views in nine of ten patients. In one patient, only scoliosis was observed on the frontal view. The abnormal pedicle was consistently present at the apex of the concavity of the curve, and in one patient, lumbar hyperlordosis was evident on the lateral view (Figs. 1a and 2a).

Table 1 Clinical and magnetic resonance imaging (MRI) features

Case	Age/ gender	Nidus level on CT	MRI			
			Spinal canal or neural foramen involvement	Extent of oedema	No. of levels of oedema	Nidus identifiable
1	12/F	L4–Rt. IAP	No	Pedicle, lamina and PLVB of L4 and L5	2	Yes
2	10/F	T6–Lt. PLVB cortex	No	Lt. pedicle and PLVB	1	Yes
3	59/M	T9–Lt. pedicle	Oedema in Lt. epidural fat and exit foramen	T9–Lt. pedicle and PLVB	1	Yes
4	14/F	L3–base of spinous process	Oedema in posterior epidural fat	Spinous process of L3	1	Yes
5	22/M	T9–Lt. SAP	No	Lt. T8, T9 pedicles and Lt. PLVB T9	2	No
6	8/F	T12–Rt. PLVB cortex	Rt. T12 exit foramen narrowing due to oedema	Rt. pedicle T12, PLVB of T12 and Rt. pedicle of L1	2	Yes
7	15/M	T9 –Lt. lamina	No	T9–Lt. pedicle, PLVB and T10–Lt. lamina and Lt. SAP.	2	Yes
8	21/F	T5–Rt. transverse process	No	Rt. transverse process	1	No
9	18/M	T11–Rt. pedicle	Narrowing Rt. exit foramen due to oedema	Rt. pedicle and PLVB	1	Yes
10	22/M	T7–Rt. lamina	No	Rt. pedicle, lamina and PLVB	1	No
11	25/F	L3–Lt. IAP	No	Lt. pedicle, spinous process and PLVB	1	No
12	13/M	L3–Rt. lamina	No	Rt. pedicle, lamina and PLVB	1	No
13	19/M	L4–Rt. lamina	No	Rt. pedicle, lamina and PLVB	1	Yes

CT computed tomography, *PLVB* posterolateral vertebral body, *Rt.* right, *Lt.* left; *N/A* not available, *IAP* inferior articular process, *SAP* superior articular process

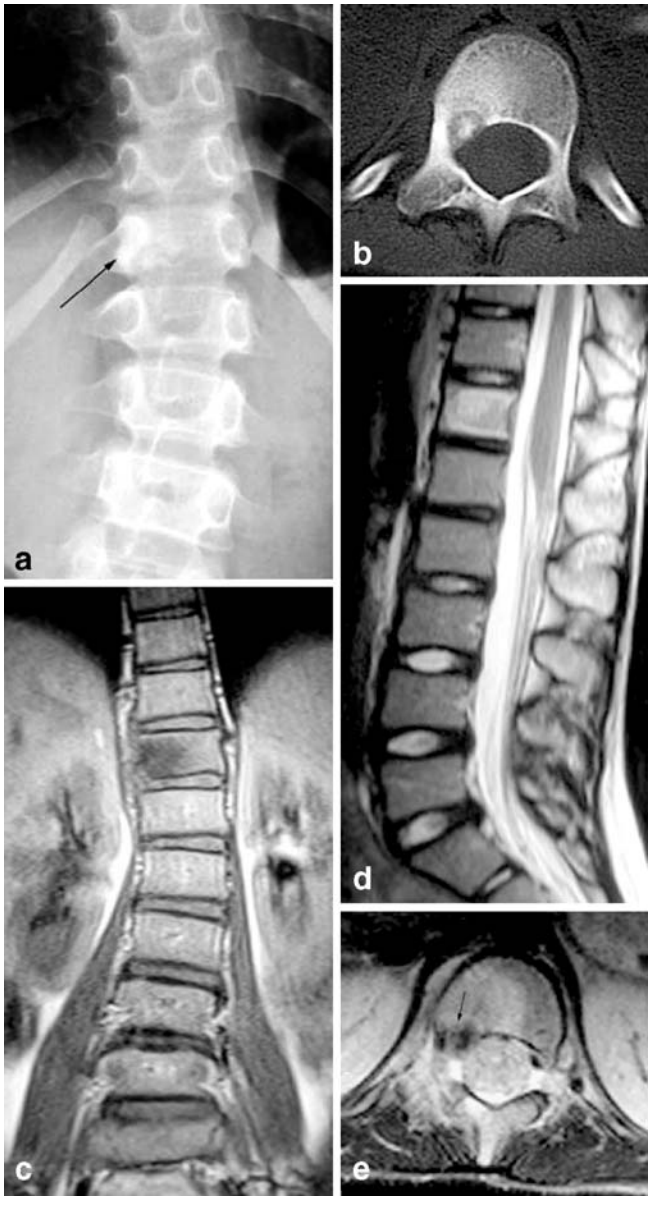

Fig. 1 Osteoid osteoma (OO) of T12. **a** Anterior posterior radiograph demonstrates a sclerotic right T12 pedicle (*arrow*). **b** Computed tomography (CT) shows the mineralised nidus at the junction of the right pedicle and the posterior vertebral body cortex. Note the reactive medullary sclerosis. **c** Coronal T1-weighted spin-echo (SE) magnetic resonance imaging (MRI) showing reduced medullary signal intensity (SI) in the right half of the T12 vertebral body due to a combination of oedema and sclerosis. Note its location on the concavity of the apex of the scoliotic curve. **d** Sagittal T2-weighted fast-spin-echo (FSE) MRI showing increased medullary SI in the T12 vertebral body due to reactive oedema. **e** Axial T2-weighted FSE MRI showing increased medullary SI in the posterolateral T12 vertebral body. The nidus (*arrow*) is hypointense

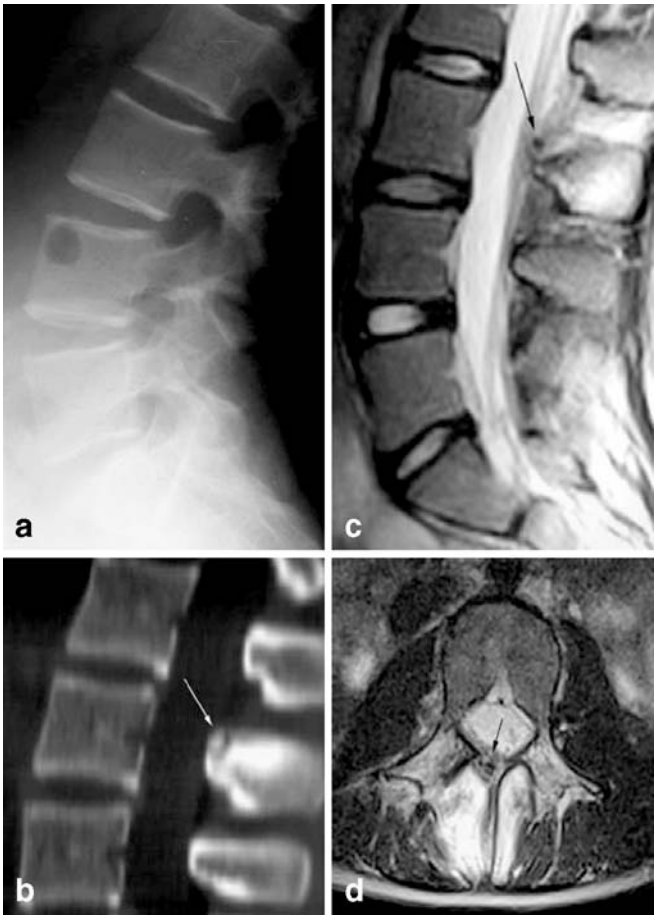

Fig. 2 Osteoid osteoma (OO) of the spinous process of L3. **a** Lateral radiograph shows lumbar hyperlordosis. **b** Sagittal multiplanar reformatting (MPR) computed tomography (CT) demonstrates the calcified nidus (*arrow*) in the superior aspect of the base of the L3 spinous process. **c** Sagittal T2-weighted fast-spin-echo (FSE) magnetic resonance imaging (MRI) showing increased medullary signal intensity (SI) in the L3 spinous process. The vertebral body marrow SI is normal. The nidus (*arrow*) appears as a low SI lesion with central signal void due to calcification. **d** Axial T2-weighted FSE MRI showing increased soft tissue SI in the posterior paraspinal muscles. The nidus (*arrow*) appears hypointense

99^{m}-Tc MDP bone scintigraphy

Focal increased uptake due to avid radionuclide accumulation consistent with a diagnosis of OO was seen in the five patients where scintigraphy was available (Fig. 3a).

Computed tomography

The nidus was demonstrated clearly in all 13 cases (Figs. 1b, 2b, 4a, 5a,b and 6a). The nidus was located in the neural arch (pedicle, lamina or articular processes in nine cases; spinous process and transverse process in one case each) or the posterior aspect of the vertebral body (two

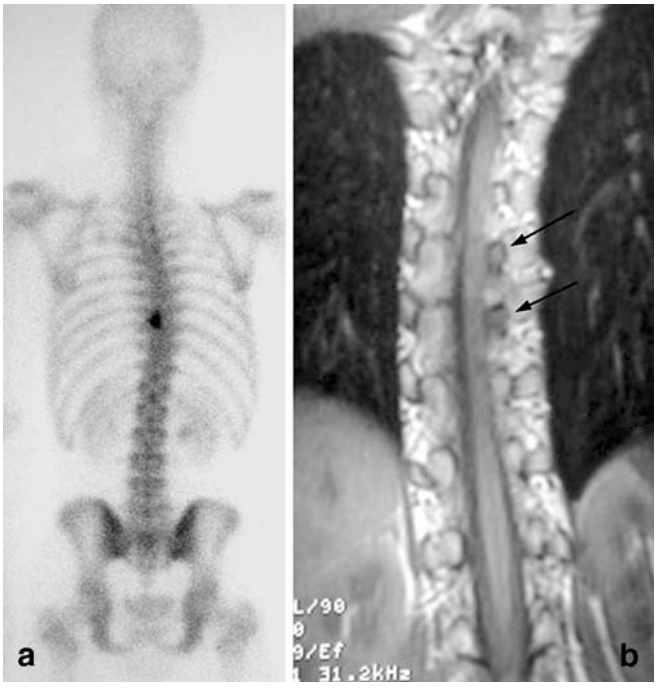

Fig. 3 Osteoid osteoma (OO) of T9. **a** Posterior view 99m-Tc MDP bone scan showing the characteristic pattern of activity with OO. **b** Coronal T1-weighted spin echo (SE) magnetic resonance imaging (MRI) showing reduced medullary signal intensity (SI) in the left T9 and T10 pedicles (*arrows*)

cases). Perinidal sclerosis accompanied the nidus in all cases except one. In this patient, the location of the nidus was in the right transverse process of T5.

Magnetic resonance imaging

The nidus was identifiable in eight cases, typically showing intermediate signal intensity (SI) on T1-weighted SE sequences and hypointensity on T2-weighted FSE sequences. Focal signal void due to matrix mineralisation was also occasionally evident (Figs. 1e, 2c,d, 5d and 6b). In the single case where gadolinium was given, perinidal enhancement of marrow oedema was noted. Oedema was classed as grade 4 in all cases. The epicentre of the oedema was in the region of the pedicle in 11 of the 13 patients. In one patient, oedema was seen predominantly in the transverse process, and in the spinous process in another patient. In the 11 cases where marrow oedema was centred around the pedicle region, the oedema classically extended anteriorly into the vertebra involving the posterior ipsilateral one third to two thirds of the vertebral body (Figs. 1c–e, 4b–c and 5c–d). In four patients, oedema was seen at two levels (Figs. 3b and 7), also involving the neural arch of an adjacent vertebra. Involvement of the spinal canal was limited to oedema in the epidural fat in two patients (Figs. 5d and 8) and involvement of ipsilateral neural exit foramen in three patients (Figs. 8 and 9). No reactive soft-tissue mass causing

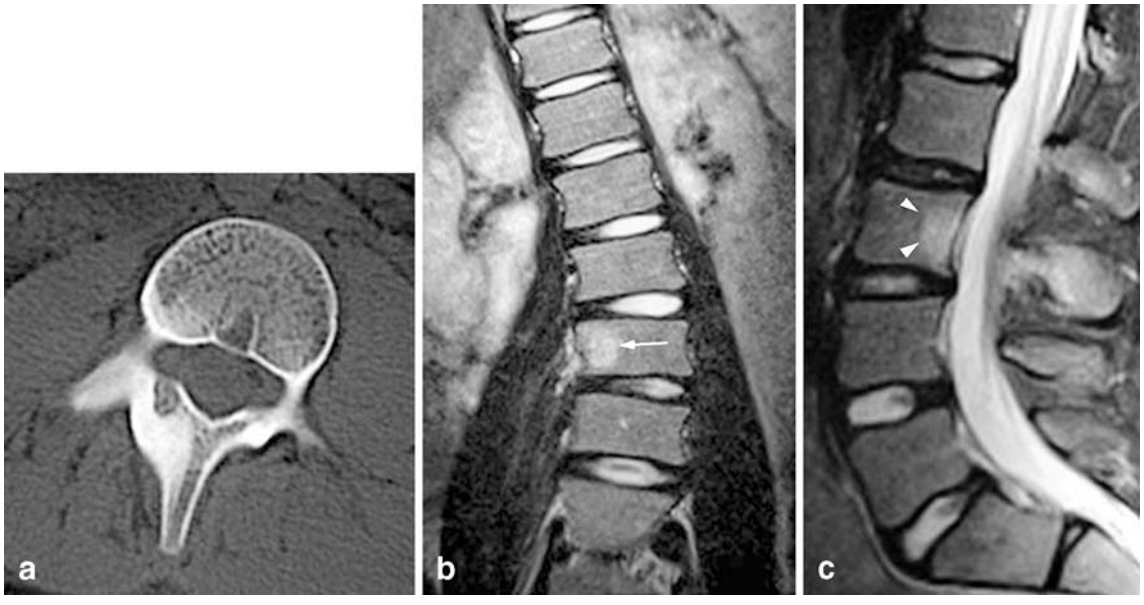

Fig. 4 Osteoid osteoma (OO) of the right lamina of L3. **a** Computed tomography (CT) showing the calcified nidus with extensive reactive cortical sclerosis. **b** Coronal T2-weighted fast-spin-echo (FSE) magnetic resonance imaging (MRI) shows increased medullary signal intensity (SI) in the right side of the L3 vertebral body (*arrow*). Note its location on the concavity at the apex of the curve. **c** Sagittal T2-weighted FSE MRI showing increased medullary SI in the posterior third of the L3 vertebral body (*arrowheads*)

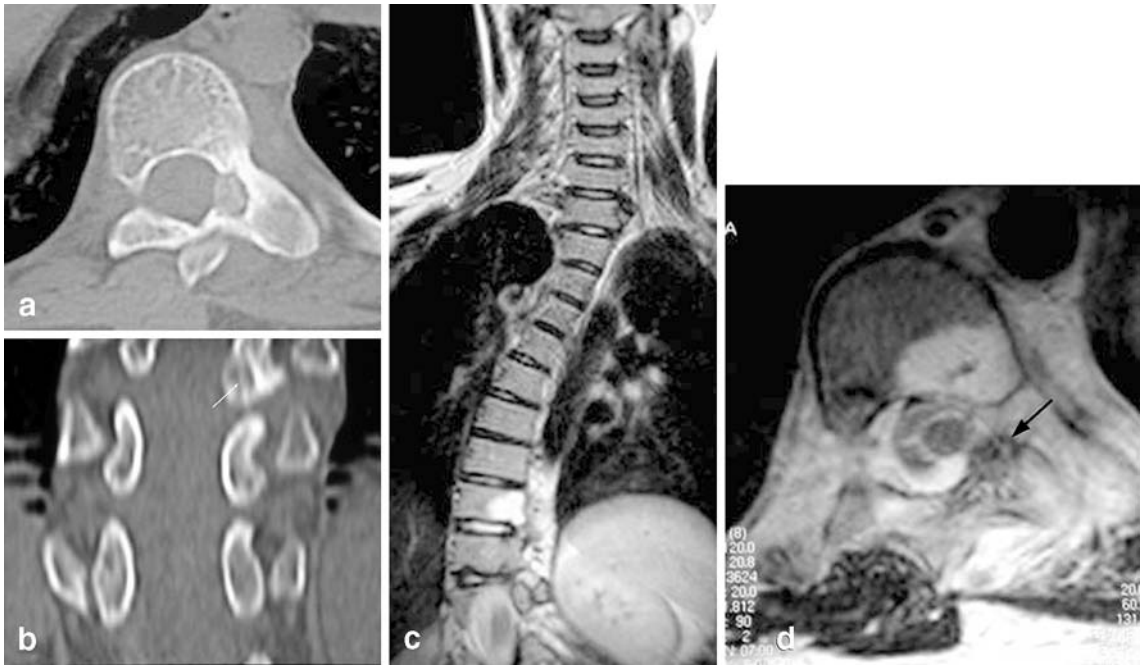

Fig. 5 Osteoid osteoma (OO) of the left pedicle of T9. **a** Computed tomography (CT) shows mineralised nidus in the inferomedial aspect of the left pedicle of T9. **b** Coronal multiplanar reformatting (MPR) CT showing the nidus (*arrow*) projecting into the foramen and causing foraminal stenosis. **c** Coronal T2-weighted fast-spin-echo (FSE) magnetic resonance imaging (MRI) showing oedema in the left side of the T9 vertebral body at the apex of the concavity of the curve. **d** Axial T2-weighted FSE MRI shows extensive medullary oedema in the neural arch and posterolateral vertebral body. The nidus is hypointense (*arrow*)

compromise of the central canal was seen in any patient. The facet joints and adjacent intervertebral discs were normal in all patients.

Discussion

OO was first described in 1935 as a distinct pathological diagnosis [6]. Approximately 90% of cases occur in patients younger than 25 years of age. Ten to twenty percent of OO occurs in the spine, with the commonest location being the lumbar vertebrae (59%), and in majority of the cases, the nidus is located in the neural arch [2, 7, 8].

The classical clinical presentation of spinal OO is that of painful scoliosis. Other clinical features include nerve root irritation and night pain. Pain relief with aspirin is classical [2, 9]. However, the typical symptoms of OO are reported to occur only in one half to two thirds of patients [10]. In particular, in the axial skeleton, the classical history may not always be elicited, leading to long diagnostic delays of up to 1–2 years, especially if the nidus is in sites of such complex anatomy as the spine [2, 11]. Spontaneous resolution of OO, which occurred in one of our cases, has been previously reported [12, 13]. Although the natural history of OO is not fully understood, it appears to be of growth followed by eventual regression in a variable period, and it does not generally grow beyond 1cm. in size [14, 15].

In most case of spinal OO, radiographs demonstrate an area of neural arch sclerosis at the apex of the concavity of a scoliosis. In the thoracic region particularly, the nidus is usually not evident [16–18]. Asymmetric muscle spasm is thought to be the cause of scoliosis [16]. The complex anatomy of the spine makes it much more difficult to detect and localise OO on radiographs compared with a location in a long bone, such as the tibia [2]. Radiographs are normal in a small number of cases of spinal OO and are often inadequate for the localisation of OO [10, 19]. In a previous report on axial OO, all the radiographs were considered to be normal [2]. However, in our series, where radiographs had been performed, features consistent with OO were present in almost all patients.

Bone scintigraphy has been advocated to localise the vertebral level in young patients with clinically suspected OO, with subsequent targeted CT examination to define the nidus. Bone scintigraphy in cases of OO is almost invariably positive [10, 20]. This was true in our cases where scintigraphy had been performed. However, spondylolysis is also an important cause of back pain in young people and can cause increased uptake on the delayed phase. It may be necessary to perform triple-phase imaging to distinguish it from OO, which typically has avid uptake on triple-phase scintigraphy due it its vascular nature [10].

The choice of imaging technique to evaluate the presence of a solitary bone lesion depends on its accuracy,

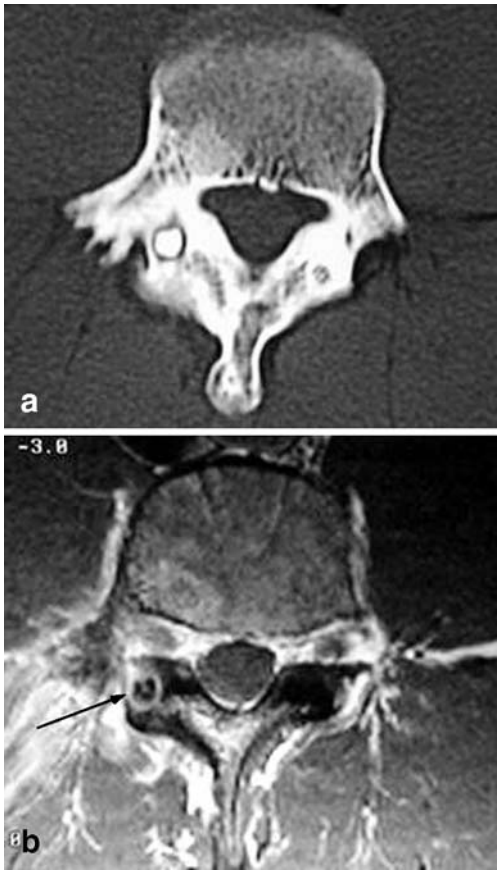

Fig. 6 Osteoid osteoma (OO) of L4. **a** Computed tomography (CT) shows a heavily calcified nidus in the right lamina. (**b**) Axial T1-weighted spin-echo (SE) magnetic resonance imaging (MRI) showing the nidus (*arrow*) with extensive internal signal void due to calcification

clinical acceptance and influence on treatment options [21]. CT has been considered the investigation method of choice to demonstrate and localise OO, and MRI has been considered to produce misleading appearances and cause diagnostic errors due to presence of associated soft tissue mass, bone marrow oedema and joint effusion [22, 23]. However, some authors recommend routine pre-operative imaging of spinal OO with CT and MRI in all cases [8]. The characteristic appearances of OO on CT are the presence of low-attenuation nidus with central mineralisation and varying degrees of perinidal sclerosis [2]. Although absence of histological proof of OO in seven cases is a slight drawback of our study, in all our cases, the nidus was definitively demonstrated on CT, and perinidal sclerosis was seen in 12 of 13 patients.

The diagnosis of spinal OO is relatively straightforward when classical symptoms are present along with positive radiographs. In these cases, CT is probably the preferred examination method to confirm the diagnosis and localise the lesion prior to treatment. However, in children and young adults, when there are no classical clinical features,

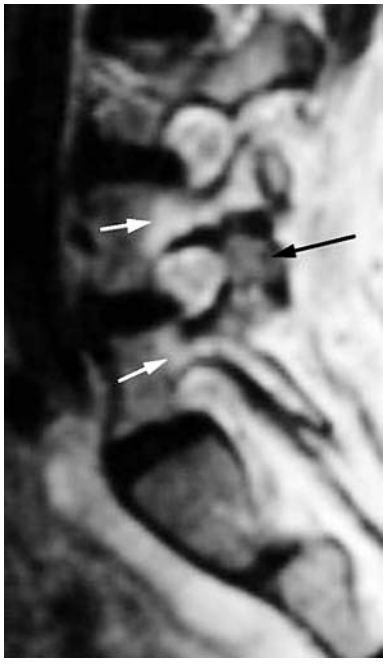

Fig. 7 Osteoid osteoma (OO) of the right lamina of L4. Sagittal T2-weighted fast-spin-echo (FSE) magnetic resonance imaging (MRI) shows oedema at the L4 and L5 levels (*white arrows*) and the low-signal-intensity (SI) nidus (*black arrow*)

MRI is usually the next investigation method following plain radiography [24–26]. Also, MRI is required to specifically document the effect of the lesion on the spinal

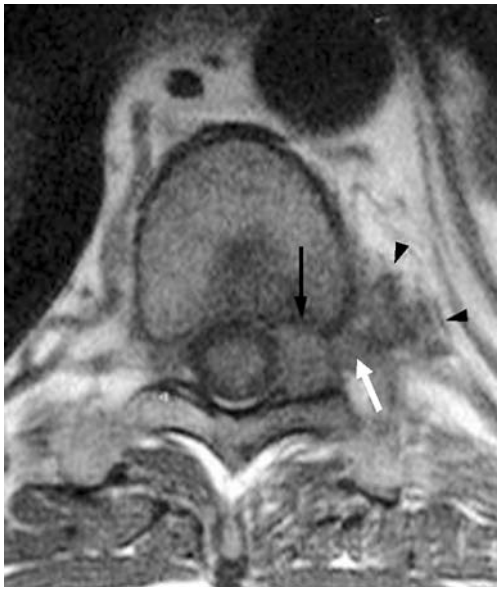

Fig. 8 Osteoid osteoma (OO) of the left pedicle of T9. Axial T1-weighted spin-echo (SE) magnetic resonance imaging (MRI) showing the intermediate-signal-intensity (SI) nidus (*black arrow*), oedema in the exit foramen (*white arrow*) and poorly defined oedema in the paravertebral fat (*arrowheads*)

Fig. 9 Osteoid osteoma (OO) of the right pedicle of T11. Axial T1-weighted magnetic resonance imaging (MRI) shows the oedema in the exit foramen on the right side (*arrow*)

canal and cord [11]. Hence, it is very important to recognise the MRI features of spinal OO.

The nidus of an OO can have a very heterogeneous, variable appearance on MRI, making characterisation difficult [22, 27, 28]. Gadolinium administration has been suggested to improve conspicuity and detection of the nidus [4, 22, 29]. In addition, dynamic gadolinium-enhanced MRI has been shown to demonstrate OO with increased conspicuity compared with non-enhanced MRI [4]. In only one of our cases was gadolinium administered, with the demonstration of perinidal enhancement. However, the nidus was also visible on axial T2-weighted image in this case as a low SI lesion surrounded by high SI oedema. In the eight cases where a nidus was identifiable in our series, it was most conspicuous on axial T2-weighted images, as the oedema served to demarcate the lesion, facilitating detection of the nidus. The nidus typically showed low SI on T2-weighted and intermediate SI on T1-weighted images. Focal signal void due to matrix mineralisation was occasionally evident.

The presence of extensive perinidal oedema in OO is thought be due to high levels of cyclo-oxygenase–2 expression in neoplastic osteoblasts in the nidus [30]. The presence of widespread sclerotic changes around the nidus in vertebrae adjacent to the one that harbours the nidus has been reported on CT [31, 32]. In four of our cases, similar changes of oedema were noted on MRI, indicating that perinidal inflammatory changes can be present at multiple levels in spinal OO. Similar features have been reported with spinal osteoblastoma [28]. Whilst some studies have suggested an inverse relationship of perinidal oedema to the age of the patient and use of aspirin, others have not found such a correlation [5, 22, 33]. No significant relationship has been proven between oedema and duration of symptoms [5]. These aspects were not assessed in our study. The possibility that vertebral lesions cause a higher grade of oedema has been suggested in a previously reported series of spinal OO [5]. The authors of that study postulated that this is due to the increased vascularity of the vertebrae and suggested that a larger series of spinal OO on MRI needed to be studied to confirm this [5]. In our study, there was grade 4 oedema in all cases, and in 11 of the 13 cases, there was an extensive pattern of oedema in the region of the pedicle classically extending anteriorly to involve the posterolateral aspect of the vertebral body to a varying degree. In all of these 11 cases, the nidus was located in the pedicle, lamina or articular facet.

Marrow oedema in the pedicle and vertebral body are by no means specific for OO. There is a differential diagnosis, including degenerative disc and facet joint disease, spondylolysis and pediculolysis [34]. Degenerative disc disease can cause oedema-type changes in the vertebral end-plates [35]. However, this usually is not extensive enough to extend to the pedicles. In none of our cases was the disc abnormal. Also, OO tends to occur in the younger age group where degenerative disc disease is rare. Pedicle marrow oedema can occur as a reactive change in patients with adjacent pars defects or due to pediculolysis [36–38]. However, in our experience, extension into the adjacent vertebral body is not a feature in these cases. Misinterpretation of the changes of marrow oedema due to OO as malignancy or previous trauma can be minimised by recognition of the characteristic findings on MRI and by interpreting MRI in conjunction with other available images [39].

In conclusion, a review of 13 cases of spinal OO has demonstrated certain characteristic MRI findings that should raise suspicion of the diagnosis. The most important is oedema in the pedicle and lamina extending anteriorly to involve a third to two thirds of the posterolateral vertebral body. It is possible to see oedema in the neural arch at an adjacent level to that which harbours the nidus. On non-enhanced MRI, the nidus is optimally visualised on T2-weighted sequences, when it appears as a hypointense lesion surrounded by marrow oedema.

References

1. Ozaki T, Liljenqvist U, Hillmann A et al (2002) Osteoid osteoma and osteoblastoma of the spine: experiences with 22 patients. Clin Orthop Relat Res 397:394–402
2. Gamba JL, Martinez S, Apple J, Harrelson JM, Nunley JA (1984) Computed tomography of axial skeletal osteoid osteomas. Am J Roentgenol 142:769–772
3. Pettine KA, Klassen RA (1986) Osteoid-osteoma and osteoblastoma of the spine. J Bone Joint Surg Am 68:354–361

4. Liu PT, Chivers FS, Roberts CC, Schultz CJ, Beauchamp CP (2003) Imaging of osteoid osteoma with dynamic gadolinium-enhanced MR imaging. Radiology 227:691–700
5. Ehara S, Rosenthal DI, Aoki J et al (1999) Peritumoral edema in osteoid osteoma on magnetic resonance imaging. Skelet Radiol 28:265–270
6. Jaffe HL (1935) "Osteoid osteoma". A benign osteoblastic tumor composed of osteoid and atypical bone. Arch Surg 31:709–728
7. Jackson RP, Reckling FW, Mants FA (1977) Osteoid osteoma and osteoblastoma. Similar histological lesions with different natural histories. Clin Orthop Relat Res 128:303–313
8. Zileli M, Cagli S, Basdemir G, Ersahin Y (2003) Osteoid osteomas and osteoblastomas of the spine. Neurosurg Focus 15:E5
9. Swee RG, McLeod RA, Beabout JW (1979) Osteoid osteoma: detection, diagnosis and localisation. Radiology 130:117–123
10. Wells RG, Miller JH, Sty JR (1987) Scintigraphic patterns in osteoid osteoma and spondylolysis. Clin Nucl Med 12:39–44
11. Scuotto A, Accardo C, Rotondo M et al (2002) Unusual manifestation of vertebral osteoid osteoma: case report. Eur Radiol 12:109–112
12. Sherman MS (1947) Osteoid osteoma: review of literature and report of 30 cases. J Bone Joint Surg 29:918–930
13. Flaherty RA, Pugh DG, Dockerty MB (1956) Osteoid osteoma. Am J Roentgenol 76:1041–1051
14. Cassar-Pullicino VN, McCall IW, Wan S (1992) Intra-articular osteoid osteoma. Clin Radiol 45:153–160
15. Cantwell CP, Obyrne J, Eustace S (2004) Current trends in treatment of osteoid osteoma with an emphasis on radiofrequency ablation. Eur Radiol 14:607–617
16. Saifuddin A, White J, Sherazi Z et al (1998) Osteoid osteoma and osteoblastoma of the spine. Factors associated with the presence of scoliosis. Spine 23:47–53
17. Metha MH, Murray RO (1977) Scoliosis provoked by painful vertebral lesions. Skelet Radiol 1:223–230
18. Ransford AO, Pozo JL, Hutton PAN et al (1984) The behavioural pattern of scoliosis associated with osteoid osteoma or osteoblastoma of the spine. J Bone Joint Surg Br 66:16–20
19. Klein MH, Shankman S (1992) Osteoid osteoma: radiologic and pathologic correlation. Skelet Radiol 21:23–31
20. Lisbona R, Rosenthal L (1979) Role of radionuclide imaging in osteoid osteoma. Am J Roentgenol 132:77–80
21. Sundaram M, McGuire M (1988) Computed tomography or magnetic resonance for evaluating solitary tumour or tumour-like lesions of bone? Skelet Radiol 17:392–395
22. Assoun J, Richardi G, Railhac JJ et al (1994) Osteoid osteoma: MR imaging versus CT. Radiology 191:217–223
23. Nogues P, Marti-Bonmati L, Aparisi F, Saborido MC, Garci J, Dosda R (1998) MR imaging assessment of juxta cortical edema in osteoid osteoma in 28 patients. Eur Radiol 8:236–238
24. Bohndorf K, Reiser M, Lochner B et al (1986) Magnetic resonance imaging of primary tumours and tumour-like lesions of bone. Skelet Radiol 15:511–517
25. Stoller DW (1989) Magnetic resonance imaging in orthopaedics and rheumatology. Lippincott, Philadelphia
26. Zimmer WD, Berquist TH, McLeod RA et al (1985) Bone tumors: magnetic resonance imaging versus computed tomography. Radiology 155:709–718
27. Davies M, Cassar-Pullicino VN, Davies AM, McCall IW, Tyrrell PN (2002) The diagnostic accuracy of MR imaging in osteoid osteoma. Skelet Radiol 31:559–569
28. Shaikh MI, Saifuddin A, Pringle J, Natali C, Sherazi Z (1999) Spinal osteoblastoma: CT and MR imaging with pathological correlation. Skelet Radiol 28:33–40
29. Youssef BA, Haddad MC, Zahrani A et al (1996) Osteoid osteoma and osteoblastoma: MRI appearances and the significance of ring enhancement. Eur Radiol 6:291–296
30. Kawaguchi Y, Hasegawa T, Oka S et al (2001) Mechanism of intramedullary high intensity area on T2-weighted magnetic resonance imaging in osteoid osteoma: a possible role of COX-2 expression. Pathol Int 51:933–937
31. Lundeen MA, Herring JA (1980) Osteoid-osteoma of the spine: sclerosis in two levels. A case report. J Bone Joint Surg Am 62:476–478
32. Hermann RM, Blount WP (1961) Osteoid osteoma of the lumbar spine. J Bone Joint Surg 43:568–571
33. Spouge AR, Thain LM (2000) Osteoid osteoma: MR imaging revisited. Clin Imaging 24:19–27
34. Morrison JL, Kaplan PA, Dussault RG, Anderson MW (2000) Pedicle marrow signal intensity changes in the lumbar spine: a manifestation of facet degenerative joint disease. Skelet Radiol 29:703–707
35. Modic MT, Steinberg PM, Ross JS, Masaryk TJ, Carter JR (1988) Degenerative disk disease: assessment of changes in vertebral body marrow with MR imaging. Radiology 166:193–199
36. Ulmer JL, Elster AD, Mathews VP, Allen AM (1995) Lumbar spondylolysis: reactive marrow changes seen in adjacent pedicles on MR images. Am J Roentgenol 164:429–433
37. Sirvanci M, Ulusoy L, Duran C (2002) Pedicular stress fracture in lumbar spine. Clin Imaging 26:187–193
38. Parvataneni HK, Nicholas SJ, 5McCance SE (2004) Bilateral pedicle stress fractures in a female athlete: case report and review of the literature. Spine 29:E19–E21
39. Woertler K (2003) Benign bone tumors and tumor-like lesions: value of cross-sectional imaging. Eur Radiol 13:1820–1835